

Augmented space recursion for partially disordered systems.

Atisdipankar Chakrabarti and Abhijit Mookerjee

S. N. Bose National Centre for Basic Sciences. Block-JD, Sector-III, Kolkata-700098, India.

E-mail: adc@boson.bose.res.in

E-mail: abhijit@boson.bose.res.in

Abstract. Off-stoichiometric alloys exhibit partial disorder, in the sense that only some of the sublattices of the stoichiometric ordered alloy become disordered. This paper puts forward a generalization of the augmented space recursion (ASR) introduced earlier by one of us (Mookerjee *et al* 1997(*)) for systems with many atoms per unit cell. In order to justify the convergence properties of ASR we have studied the convergence of various moments of local density of states and other physical quantities like Fermi energy and band energy. We have also looked at the convergence of the magnetic moment of Ni, which is very sensitive to numerical approximations towards the k -space value $0.6 \mu_B$ with the number of recursion steps prior to termination.

PACS numbers: 71.20,71,20c

Submitted to: *J. Phys.: Condens. Matter*

1. Introduction

Binary alloys in stoichiometric compositions invariably exhibit ordered structures at low temperatures. As we depart from perfect stoichiometric compositions, it is not possible to populate the lattice in the given compositions so as to produce a perfectly ordered structure. Take for example, a $B_{75}A_{25}$ binary alloy on an fcc lattice. One of the possible stable ordered phases is the L12 arrangement as shown in figure 1. An example of this is Cu_3Au . In a cubic unit cell the corner is occupied by an A atom, while the three face centres by B atoms. Since there are N corners and $3N$ face centres (N being the total number of unit cells in the solid) and exactly as many A and B atoms, at this composition the L12 ordered arrangement exactly populates all the lattice sites. Ordered arrangement becomes impossible, say for $B_{70}A_{30}$. However, the following arrangement becomes possible : since there are now $1.2N$ A atoms, N of them may occupy the N corners. The $3N$ face centres may be occupied randomly by the $2.8N$ B atoms and $0.2N$ remaining A atoms. The original A sublattice remains ordered, while the B sublattice becomes disordered. Since there are on the whole $3N$ face centres, the occupation probability of the A and B atoms in this sublattice are $0.9\bar{3}$ and $0.0\bar{6}$ respectively. This arrangement is quite different from the completely random alloy, where all sites are randomly occupied by either the A or B atom with probabilities 0.3 and 0.7 respectively. It is also rather different from the *partial disorder* defined by [10]. In this communication we shall define *partial disorder* in the manner described above.

The recursion method was introduced by [6, 7] as a convenient and numerically efficient method for calculating Green functions and realistic physical properties like the local density of states (LDOS), the Fermi energy and the band energy. The method comes to its own in situations where translation symmetry of the potential in an effective one-

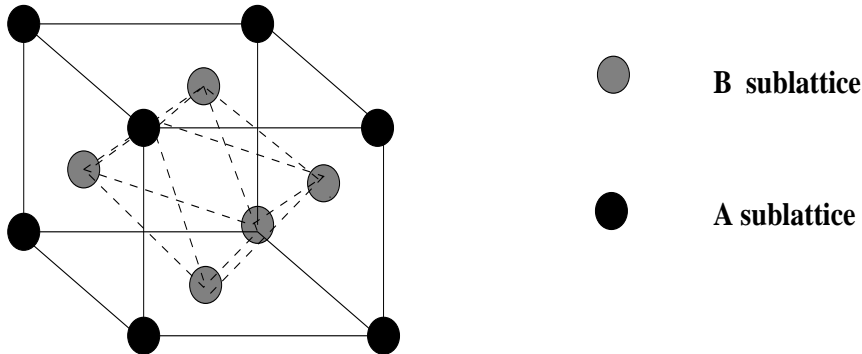


Figure 1. The L12 atomic arrangement for 75-25 AB binary alloys on a fcc lattice

electron Hamiltonian is lost. The Bloch Theorem is violated, and we cannot employ the standard reciprocal space techniques unless we carry out a homogeneity restoring mean-field approximation (like the coherent potential approximation, CPA). This can happen, for instance, at a surface or in a random alloy. In particular, if the ion-cores sit on a topologically distorted network or at a rough surface or interface, where the recursion method seems the only natural way of dealing with electronic property calculations.

There exists a large body of literature on the application of the recursion method to various situations ([8]). For substitutional disorder, the recursion method has been employed in tandem with the augmented space formalism ([11, 12, 13, 14, 15]) (augmented space recursion or ASR) for dealing with random alloys, taking into account local configuration fluctuations like chemical clustering, local lattice distortions due to size effects and inhomogeneous randomness at a surface because of surface segregation. In spite of this extensive body of literature, the recursion method does not seem to have gained wide acceptability in the electronic structure community, and one often has had to face skepticism regarding its accuracy and feasibility when applied with sophisticated electronic structure techniques to realistic systems.

In this communication we shall first present the ASR in detail for the most general case of systems with many atoms per unit cell. Our subsequent aim will be to study partially disordered systems in alloys with off-stoichiometric compositions.

We shall carry out recursion calculations based on the tight-binding linearized muffin-tin orbitals (TB-LMTO) method ([1, 2, 3]) for various metals and alloys, to start with for perfectly ordered systems, compare them with standard reciprocal space methods also based on the TB-LMTO and then carry out a thorough analysis of the convergence and accuracy of the technique. The aim will be to have a convincing handle on the possible errors in the method with a view to minimizing them within our tolerance limits. Having convinced ourselves about the feasibility of the method, we shall first apply it to a toy model for partial disorder before carrying on to realistic systems.

2. Formalism

2.1. Generalized Augmented Space Recursion within the TB-LMTO formalism.

In earlier works ([13, 14, 15]) it has been established that for a disordered system the Augmented Space Theorem maps a disordered Hamiltonian described in a Hilbert space H onto an ordered Hamiltonian in an enlarged space Ψ , where the space Ψ is constructed by augmenting the configuration space Φ of the random variables of the disordered Hamiltonian together with the Hilbert space H of the disordered Hamiltonian. Thus $\Psi = \Phi \otimes H$. The configuration average of the Green function reduces to the evaluation of a particular matrix element of the resolvent of this enlarged Hamiltonian in the augmented space. Hence, if one performs a recursion in the augmented space, one can obtain the matrix element necessary to calculate the configuration average of a Green

function directly. The advantage of this method is that it does not involve a single site approximation or the solution of any self-consistent equation (which is a prerequisite for the CPA or its generalizations). Furthermore, one can treat both diagonal and off-diagonal disorder on an equal footing. In spite of its immense potential, the method could not be implemented in a real alloy systems successfully earlier because of the large rank of the augmented Hamiltonian. For a binary alloy with N sites and with only s -orbitals it is $N \times 2^N$). However, if we exploit the symmetry of the augmented space (which arises due to the homogeneity of the disorder) the rank of the irreducible part of the augmented space in which the recursion is effectively carried out, is considerably reduced and recursion becomes tractable. Unlike other methods like the embedded-cluster method, where the configuration averaging is done by explicit averaging over all the distinct configurations of the embedded cluster (144 for a fcc lattice with first shell of neighbours), this generalized augmented-space recursion technique yields, in a single recursion, the configuration average directly. In a recent paper, [9] has rederived the augmented space technique and related it to the idea of spatial ergodicity which connects volume averaging to configuration averaging in the infinite solid limit.

As has been mentioned earlier, since the recursion method needs a localized, short-ranged basis for its operation, one can implement augmented space recursion in the framework of the TB-LMTO formalism. We now describe the methodology of generalized augmented space recursion in the framework of the TB-LMTO.

The second order TB-LMTO Hamiltonian is written in terms of potential parameters and screened structure matrix. For a random binary alloy $A_x B_y$, the LMTO Hamiltonian in the most localized representation is given by,

$$\mathcal{H}^{(2)} = E_\nu + h - hoh \quad (1)$$

where,

$$h = \sum_{RL\alpha} \left(\tilde{\mathbf{C}}_{RL\alpha} - \tilde{\mathbf{E}}_{RL\alpha} \right) \mathcal{P}_{RL\alpha} + \sum_{RL\alpha} \sum_{R'L'\alpha'} \tilde{\Delta}_{RL\alpha}^{1/2} S_{RL\alpha, R'L'\alpha'} \tilde{\Delta}_{R'L'\alpha'}^{1/2} \mathcal{T}_{RL\alpha, R'L'\alpha'} \quad (2)$$

C , o and Δ are potential parameters of the TB-LMTO method, these are diagonal matrices in the angular momentum indices. Also o^{-1} has the dimension of energy and is a measure of the energy window around \tilde{E} around which the approximate Hamiltonian \mathcal{H}^2 is reliable.

$$\begin{aligned} \tilde{\mathbf{C}}_{RL\alpha} &= C_L^A n_R^\alpha + C_L^B (1 - n_R^\alpha) = C_L^B + \delta C_L n_R^\alpha \\ \delta C_L &= C_L^A - C_L^B \\ \tilde{\Delta}_{RL\alpha}^{1/2} &= \left(\Delta_L^A \right)^{1/2} n_R^\alpha + \left(\Delta_L^B \right)^{1/2} (1 - n_R^\alpha) = \left(\Delta_L^B \right)^{1/2} + \delta \Delta_L^{1/2} n_R^\alpha \\ \delta \Delta_L^{1/2} &= \left(\Delta_L^A \right)^{1/2} - \left(\Delta_L^B \right)^{1/2} \end{aligned}$$

$$\begin{aligned}
 \tilde{\mathbf{o}}_{RL\alpha} &= o_L^A n_R^\alpha + o_L^B (1 - n_R^\alpha) = o_L^B + \delta o_L n_R^\alpha \\
 \delta o_L &= o_L^A - o_L^B \\
 \tilde{\mathbf{E}}_{\nu RL\alpha} &= E_{\nu L\alpha}^A n_R^\alpha + E_{\nu L\alpha}^B (1 - n_R^\alpha) = E_{\nu L\alpha}^B - \delta E_{\nu L\alpha} n_R^\alpha \\
 \delta E_{\nu L\alpha} &= E_{\nu L\alpha}^A - E_{\nu L\alpha}^B
 \end{aligned}$$

R denotes a *cell position* label associated with a TB-LMTO basis and $L = (\ell m m_s)$ is the composite angular momentum index. α denotes an atom in the R -th cell whose position is $R + \xi^\alpha$. n_R^α is the site-occupation variable which takes values 0 or 1 depending upon whether site α in the R -th cell is occupied by an A or a B atom. For *partial disorder* this is a random variable whose probability density depends upon which sublattice it belongs to, hence the label α associated with it. The structure matrix $S_{RL\alpha, R'L'\alpha'}$ is non-random in case of substitutional alloys with negligible size mismatch. Now one can obtain the full \mathcal{H}^2 by inserting h in expression (1).

$\mathcal{P}_{RL\alpha}$ and $\mathcal{T}_{RL\alpha, R'L'\alpha'}$ are the projection and transfer operators in Hilbert space H spanned by tight-binding basis $\{|RL\alpha\rangle\}$.

$$\begin{aligned}
 \mathcal{P}_{RL\alpha} &= |RL\alpha\rangle\langle RL\alpha| \\
 \mathcal{T}_{RL\alpha, R'L'\alpha'} &= |RL\alpha\rangle\langle R'L'\alpha'|
 \end{aligned} \tag{3}$$

The expanded Hamiltonian $\hat{\mathcal{H}}$ in the augmented space is constructed by replacing the random site occupation variable n_R^α by its corresponding operator representation \mathcal{M}_R^α in configuration space.

$$\begin{aligned}
 \hat{\mathbf{h}} &= \sum_{RL\alpha} \left((C_L^B - E_{\nu L}^B) \hat{\mathcal{I}} + (\delta C_L - \delta E_{\nu L}) \mathcal{M}_R^\alpha \right) \otimes \mathcal{P}_{RL\alpha} + \dots \\
 &+ \sum_{RL\alpha} \sum_{R'L'\alpha'} \left((\Delta_L^B)^{1/2} \hat{\mathcal{I}} + \delta \Delta_L^{1/2} \mathcal{M}_R^\alpha \right) S_{RL\alpha, R'L'\alpha'}^\alpha \left((\Delta_{L'}^B)^{1/2} \hat{\mathcal{I}} + \delta \Delta_{L'}^{1/2} \mathcal{M}_{R'}^\alpha \right) \otimes \mathcal{T}_{RL\alpha, R'L'\alpha'}
 \end{aligned} \tag{4}$$

where, \mathcal{M}_R^α is given by

$$\mathcal{M}_R^\alpha = x_A^\alpha \mathcal{P}_{R\alpha}^\uparrow + x_B^\alpha \mathcal{P}_{R\alpha}^\downarrow + \sqrt{(x_A^\alpha x_B^\alpha)} \left(\mathcal{T}_{R\alpha}^{\uparrow\downarrow} + \mathcal{T}_{R\alpha}^{\downarrow\uparrow} \right)$$

Now inserting equation(4) in equation(1) one can obtain the full Hamiltonian $\hat{\mathcal{H}}$. This Hamiltonian is now an operator in a much enlarged space $\Psi = \Phi \otimes \mathcal{H}$ (the augmented space). The Hilbert space Ψ is spanned by the basis set $\{|R, L, \alpha, \{C\}\rangle\}$, where $\{C\}$ is a pattern $(\uparrow\uparrow\downarrow\uparrow\dots)$ spanning the configuration space and described in terms of the *cardinality sequence* $\{C\}$ of positions of the \downarrow in the pattern. The enlarged Hamiltonian does not involve any random variables but incorporates within itself the full statistical information about the random occupation variables.

In the presence of off-diagonal disorder, which is invariably present in the form of the TB-LMTO Hamiltonian, even the reduction of the rank of the invariant subspace on which recursion acts, using the symmetries of the augmented space, does not allow us to sample as many configuration states as we would like. This is because, as recursion proceeds, the number of configuration states sampled at the n -th step of recursion becomes unmanageably large when $n > 5$ (for example). To do away with this problem, the working equations are transformed so as to put the Hamiltonian for the recursion in an effective diagonal disorder form. This allows one to sample further shells in augmented-space and to confirm the shell-convergence of the recursion.

To do this, we first suppress all the indices and write the expression for the resolvent as follows :

$$\begin{aligned} (E - \mathcal{H}^{(2)})^{-1} &= (E - \tilde{\mathcal{C}} - \tilde{\Delta}^{1/2} S \tilde{\Delta}^{1/2} + h\tilde{o}h)^{-1} \\ &= \tilde{\Delta}^{1/2} \left[\frac{E - \tilde{\mathcal{C}}}{\tilde{\Delta}} - S + \left(\frac{\tilde{\mathcal{C}} - \tilde{\mathbf{E}}_\nu}{\tilde{\Delta}} + S \right) (\tilde{\Delta}^{1/2} \tilde{o} \tilde{\Delta}^{1/2}) \left(\frac{\tilde{\mathcal{C}} - \tilde{\mathbf{E}}_\nu}{\tilde{\Delta}} + S \right) \right]^{-1} \tilde{\Delta}^{1/2} \end{aligned}$$

Using the augmented space theorem, we can write the expression of configuration averaged Green function as,

$$\ll G_{RL\alpha, RL\alpha}(E) \gg = \langle R, L, \alpha, \{\emptyset\} | (E\hat{I} - \hat{\mathcal{H}})^{-1} | R, L, \alpha, \{\emptyset\} \rangle$$

where,

$$A_L^\alpha (\Delta^{-1/2}) |R, L, \alpha \otimes \{\emptyset\}\rangle + F_L^\alpha (\Delta^{-1/2}) |R, L, \alpha \otimes \{R\}\rangle = |1\rangle$$

We define $[A_L^\alpha (1/\Delta)]^{1/2} |1\rangle$ as the normalized initial recursion vector $|1\rangle$.

Finally, we arrive at the convenient expression :

$$\ll G_{RL\alpha, RL\alpha}(E) \gg = \langle 1 | [\hat{E} - \hat{A} + \hat{B} + \hat{F} - \hat{S} + (\hat{J} + \hat{S}) \hat{o} (\hat{J} + \hat{S})]^{-1} | 1 \rangle$$

where,

$$\begin{aligned} \hat{A} &= \sum_{R,L,\alpha} \left\{ \frac{A_L^\alpha (C/\Delta)}{A_L^\alpha (1/\Delta)} \right\} \mathcal{P}_{R,\alpha} \otimes \mathcal{P}_L \otimes \mathcal{I} \\ \hat{B} &= \sum_{R,L,\alpha} \left\{ \frac{B_L^\alpha ((E-C)/\Delta)}{A_L^\alpha (1/\Delta)} \right\} \mathcal{P}_{R,\alpha} \otimes \mathcal{P}_L \otimes \mathcal{P}_{R\alpha}^\dagger \\ \hat{F} &= \sum_{R,L,\alpha} \left\{ \frac{F_L^\alpha ((E-C)/\Delta)}{A_L^\alpha (1/\Delta)} \right\} \mathcal{P}_{R,\alpha} \otimes \mathcal{P}_L \otimes (\mathcal{T}_{R\alpha}^{\uparrow\downarrow} + \mathcal{T}_{R\alpha}^{\downarrow\uparrow}) \end{aligned}$$

$$\hat{S} = \sum_{RL\alpha} \sum_{R'L'\alpha'} \left\{ A_L^\alpha (1/\Delta)^{-1/2} \right\} S_{RL\alpha, R'L'\alpha'} \left\{ A_L^\alpha (1/\Delta)^{-1/2} \right\} \mathcal{T}_{R\alpha, R'\alpha'} \otimes \mathcal{T}_{LL'} \otimes \mathcal{I}$$

here, $\hat{J} = \hat{J}_A + \hat{J}_B + \hat{J}_F$ and $\hat{o} = \hat{o}_A + \hat{o}_B + \hat{o}_F$, where,

$$\begin{aligned}\hat{J}_A &= \sum_{R,L,\alpha} \left\{ \frac{A_L^\alpha ((C - E_\nu) / \Delta)}{A_L^\alpha (1/\Delta)} \right\} \mathcal{P}_{R,\alpha} \otimes \mathcal{P}_L \otimes \mathcal{I} \\ \hat{J}_B &= \sum_{R,L,\alpha} \left\{ \frac{B_L^\alpha ((C - E_\nu) / \Delta)}{A_L^\alpha (1/\Delta)} \right\} \mathcal{P}_{R,\alpha} \otimes \mathcal{P}_L \otimes \mathcal{P}_{R\alpha}^\downarrow \\ \hat{J}_F &= \sum_{R,L,\alpha} \left\{ \frac{F_L^\alpha ((C - E_\nu) / \Delta)}{A_L^\alpha (1/\Delta)} \right\} \mathcal{P}_{R,\alpha} \otimes \mathcal{P}_L \otimes (\mathcal{T}_{R\alpha}^{\uparrow\downarrow} + \mathcal{T}_{R\alpha}^{\downarrow\uparrow}) \\ \hat{o}_A &= \sum_{R,L,\alpha} \{A_L^\alpha(\tilde{o}) A_L^\alpha(1/\Delta)\} \mathcal{P}_{R,\alpha} \otimes \mathcal{P}_L \otimes \mathcal{I} \\ \hat{o}_B &= \sum_{R,L,\alpha} \{B_L^\alpha(\tilde{o}) A_L^\alpha(1/\Delta)\} \mathcal{P}_{R,\alpha} \otimes \mathcal{P}_L \otimes \mathcal{P}_{R\alpha}^\downarrow \\ \hat{o}_F &= \sum_{R,L,\alpha} \{F_L^\alpha(\tilde{o}) A_L^\alpha(1/\Delta)\} \mathcal{P}_{R,\alpha} \otimes \mathcal{P}_L (\mathcal{T}_{R\alpha}^{\uparrow\downarrow} + \mathcal{T}_{R\alpha}^{\downarrow\uparrow})\end{aligned}$$

where,

$$\begin{aligned}A_L^\alpha(Z) &= x_A^\alpha Z_L^A + x_B^\alpha Z_L^B \\ B_L^\alpha(Z) &= (x_B^\alpha - x_A^\alpha) (Z_L^A - Z_L^B) \\ F_L^\alpha(Z) &= \sqrt{x_A^\alpha x_B^\alpha} (Z_L^A - Z_L^B)\end{aligned}$$

Z is any single site parameter.

Though the computational burden is considerably reduced due to diagonal formulation, the recursion now becomes energy dependent as is clear from the expressions of \hat{B} and \hat{F} above. The old formalism was free of this constraint. This energy dependence makes the recursion technique rather unsuitable because now we have to carry out one recursion per energy point of interest. This problem is tackled using *seed recursion technique* ([4]). The idea is to choose a few seed points across the energy spectrum uniformly, carry out recursion on those points and then fit the coefficients of recursion throughout the whole spectrum. This way one can save huge computation time. For example, if one is interested in an energy spectrum of 100 points, in the bare diagonal formulation recursion has to be carried out at all the 100 points but in the seed recursion technique one needs to perform recursions only at 15-20 points. The whole idea stems from the fact that in most of the cases of binary alloys, it is seen that the recursion coefficients α_n and β_n vary quite weakly across the energy spectrum. So, one can easily pick up a few of them and fit throughout the whole range of energy by a suitable function.

2.2. Convergence of the recursion method

Before we apply the above methodology to study realistic alloy systems, we must first ensure that the technique is stable and convergent. We shall illustrate the nature of convergence of various calculated physical quantities which are basic for any electronic structure calculation. This study of convergence is essential because otherwise we will

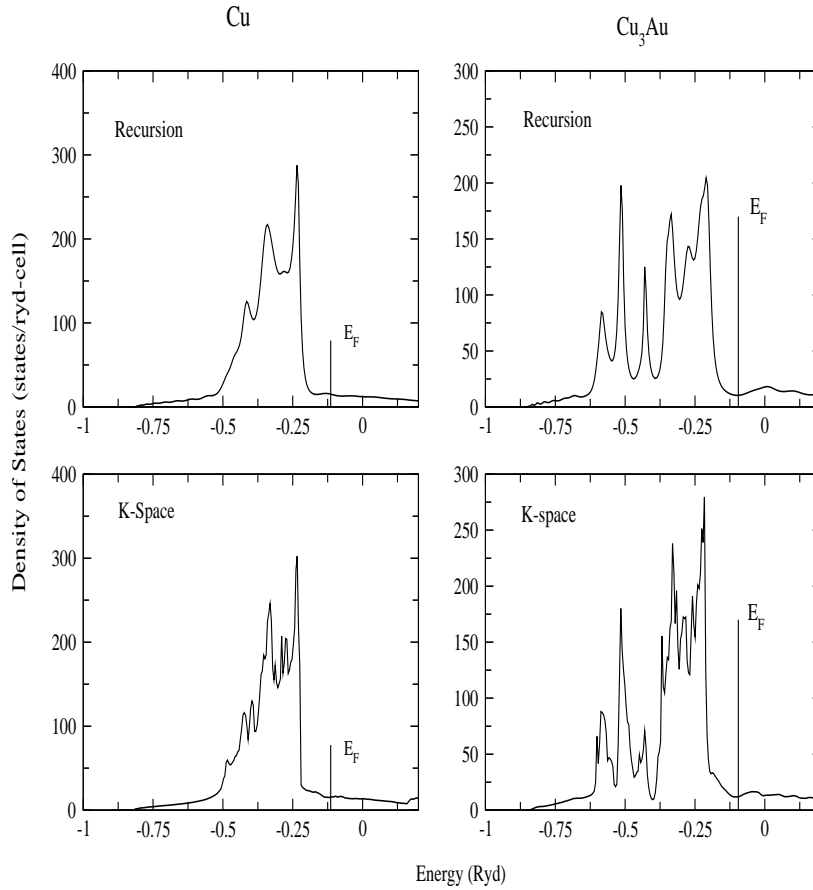


Figure 2. The Density of States for Cu and Cu₃Au using (top) the recursion method and (bottom) the k-space method

not be able to set the cut-offs of various parameters like number of shells in real and configuration spaces, recursion levels and so on, for further calculations and ensure that our numerical results are within our tolerance window.

Before we set out to analyze the errors in the method, let us first compare the results for the density of states for Cu, Cu₃Au, V and Ni as obtained from a forty-step recursion carried out on an exact twenty shell real-space map. The choice of the systems is deliberate. Cu is a full *d*-shell noble metal, V is a half-filled metal in the lower end of the transition series while Ni is a magnetic transition metal. Cu₃Au is an ordered alloy which is stable in the L12 arrangement on a fcc lattice. Figures 2 and 3 show this comparison.

For *Cu* and *Cu₃Au* most of the detailed features of the density of states calculated from

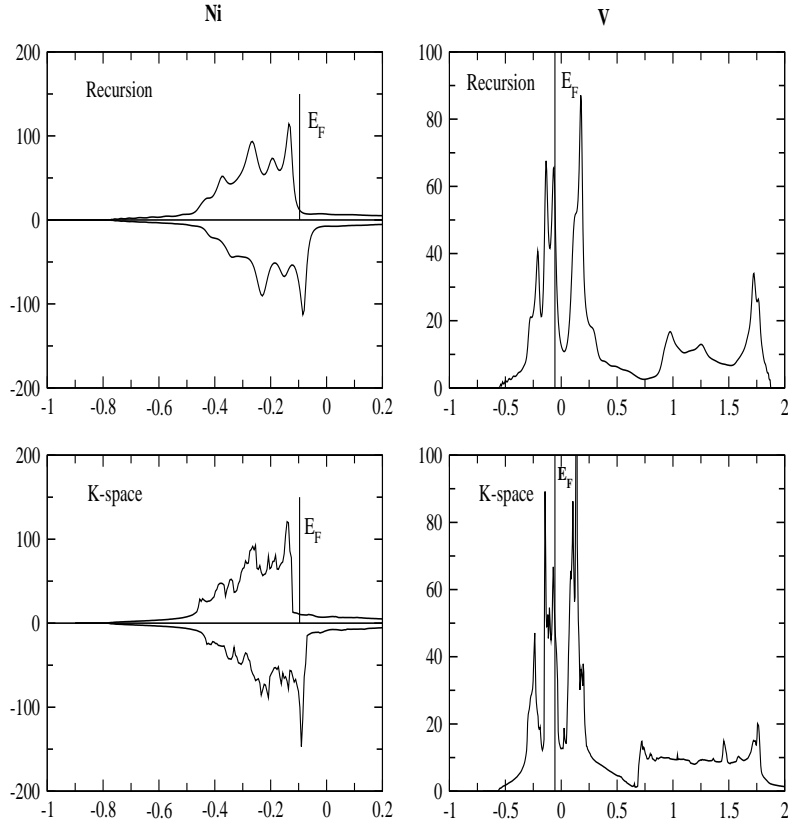


Figure 3. The Density of States for Ni and V using (top) the recursion method and (bottom) the k-space method

the recursion calculations match with the k-space results. As expected, the k-space results show sharper structures. The Fermi energies in both cases match to within a few hundredths of a rydberg. Both the majority and minority band density of states for ferromagnetic *Ni* are reproduced excellently well in the recursion calculations. The agreement is equally good for *V* upto the Fermi energy. The unoccupied part of the band shows disagreement. However, it must be understood that the recursion is done with the second order Hamiltonian in the most localized representation of the TB-LMTO, while the k-space calculations are done with the orthogonal representation. A higher order recursion calculation should improve the unoccupied part of the band considerably.

How good are our results ? When we talk of convergence of the recursion method, we have to be careful in stating precisely what we mean. Finite space approximants to Green functions do not converge for real energy values. This problem arises in every computational method, as noted by [8] . The problem definitely arises in the usual k-space integration techniques, where methods using either complex energies or

complex k -s have been attempted. The cause of this non-convergence is that an arbitrary small perturbation, like adding a single atom to a large but finite system, can shift all eigenvalues of the system. This causes an infinite change in the Green function near its corresponding poles. Thus, the precise meaning of the convergence of the recursion should imply rather the convergence of physical quantities built out of it. Most physical quantities are averages over the spectrum of the type :

$$F(E) = \int_{E_0}^{E_F} f(E') n(E') dE'$$

E_0 is the lower band edge, and $f(E)$ is any smooth, well-behaved function of E . It is the convergence of these quantities which will decide whether the recursion is convergent or not. For example, the Fermi energy is defined by

$$\int_{-E_0}^{E_F} n(E') dE' = n_e$$

where n_e is the total number of electrons. While the band energy is

$$U = \int_{-E_0}^{E_F} E' n(E') dE'$$

We shall study, in general, the convergence of indefinite integrals of the kind

$$M_k(E) = \int_{-\infty}^E (E')^k n(E') dE'$$

The integrand E'^k is monotonic and well behaved within the integration range. A measure of the root-mean-square error in the moments is

$$\Delta_k = \left\{ \frac{1}{E_U - E_0} \left(\int_{E_0}^{E_U} (\delta M_k(E))^2 dE - \left(\int_{E_0}^{E_U} \delta M_k(E) dE \right)^2 \right) \right\}^{1/2} \quad (5)$$

Errors can arise in the recursion procedure because of two distinct sources : (i) the error that arises because we carry out a finite number of recursion steps and then terminate the continued fraction using one of the available terminators ; (ii) the error that arises because we choose a large but finite part of the nearest-neighbour map and ignore the part of the augmented space very *far* from the starting state. Haydock has justified both these approximations by stating that (i) if the terminator is so chosen so as to reflect the asymptotic behaviour of the continued fraction, errors should be small, and (ii) since we can write expressions for the continued fraction in terms of self-avoiding *walks* in augmented space, long walks are dominated by those that wind round the starting state and do not go far away from it.

We shall first carry out a simple error analysis of the continued fraction expression for the Green function because of errors created on the continued fraction coefficients.

The recursion is a two-term recurrence relation. We may therefore generate from this, a pair of linearly independent set of polynomials through the relations :

$$b_{n+1}X_{n+1}(E) = (E - a_n)X_n(E) - b_nX_{n-1}$$

where, $X_n(E)$ is either $P_n(E)$ or $Q_n(E)$ according to the initial conditions :

$$\begin{aligned} P_1(E) &= 1 & P_2(E) &= (E - a_1)/b_2 \\ Q_1(E) &= 0 & Q_2(E) &= 1 \end{aligned}$$

The approximated Green function in terms of the terminator $T(E)$ is given by :

$$G(E) = \frac{Q_{N+1}(E) - b_N Q_N(E)T(E)}{b_1 [P_{N+1}(E) - b_N P_N T(E)]}$$

The terminator determines entirely the essential singularities of the the spectrum. [8] showed that a finite composition of fractional linear transformations like the one above can at most add a finite number of poles to the spectrum. The essential singularities of the exact $G(E)$ and $T(E)$ coincide. The fractional linear transformation redistributes the spectral weights over the spectrum.

Let us now assume that we make errors $\{\delta a_n, \delta b_n\}$ in the corresponding continued fraction coefficients. If we now start generating the orthogonal polynomials, starting from the exact initial conditions, but with the errors in the continued fraction coefficients, we shall obtain a pair of sets $\{\tilde{P}_n\}$ and $\{\tilde{Q}_n\}$. In general we shall have,

$$\tilde{P}_n(E) = (1 + A_n(E)) P_n(E) + B_n(E)Q_n(E)$$

If we substitute this back into the recurrence relation and keep only the first order terms in the errors,

$$\begin{aligned} A_n(E) &= \{\delta a_n [P_{n+1}(E)Q_{n+1}(E)] \\ &\quad + \delta b_n [P_n(E)Q_{n+1}(E) + P_{n+1}(E)Q_n(E)]\} / b_1 \\ B_n(E) &= \{-\delta a_n P_{n+1}(E)^2 - \delta b_n [2 P_n(E)P_{n+1}(E)]\} / b_1 \end{aligned}$$

Using the above and the expression for the local density of states , we find that the first order relative error produced in the local density of states

$$\frac{\delta n(E)}{n(E)} = -2 \left[\left\{ \sum_{n=1}^{\infty} A_n(E) \right\} + b_1 R(E) \left\{ \sum_{n=0}^{\infty} B_n(E) \right\} \right]$$

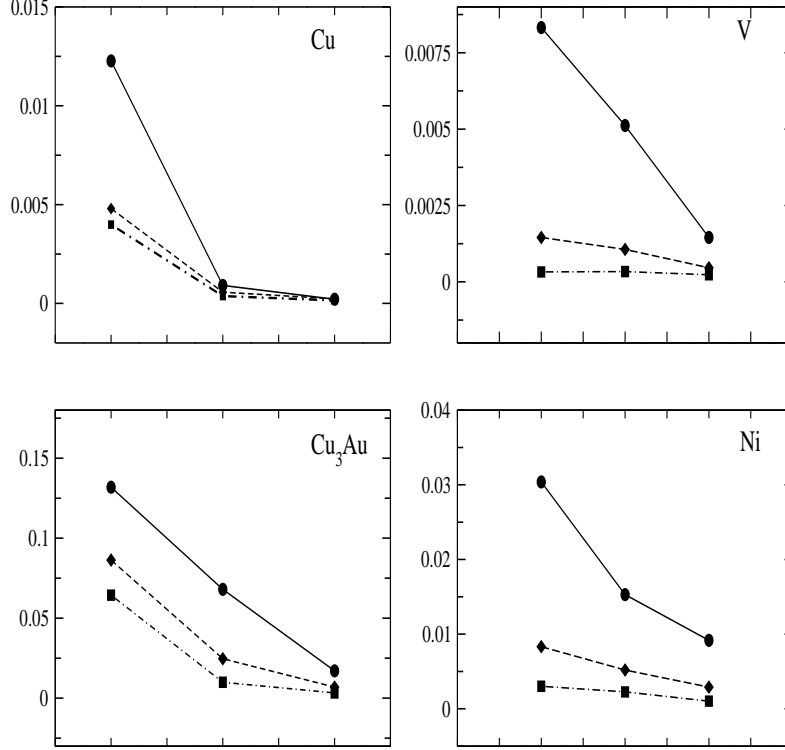


Figure 4. The root mean square errors in the first (full lines), second (dashed lines) and third (dashed dotted lines) moments of the density of states as functions of the recursion steps

where $R(E) = \mathcal{R}e G(E)$. If we define the weighted Hilbert transforms of $P_n(E)$ as the so-called associated functions :

$$\mathcal{Q}_n(E) = \mathcal{R}e \left\{ \int_{-\infty}^{\infty} \frac{P_n(E')n(E')}{E - E'} dE' \right\}$$

These associated functions are also solutions of the three-term recursion. They are not polynomials, but are nevertheless orthogonal to the set $P_n(E)$.

In terms of these, the error in the density of states is :

$$\frac{\delta n(E)}{n(E)} = \frac{2}{b_1} \left\{ \sum_{n=1}^{\infty} [\delta a_n P_{n+1}(E) \mathcal{Q}_{n+1}(E) + 2 \delta b_{n+1} P_{n+1} \mathcal{Q}_{n+2}] \right\} \quad (6)$$

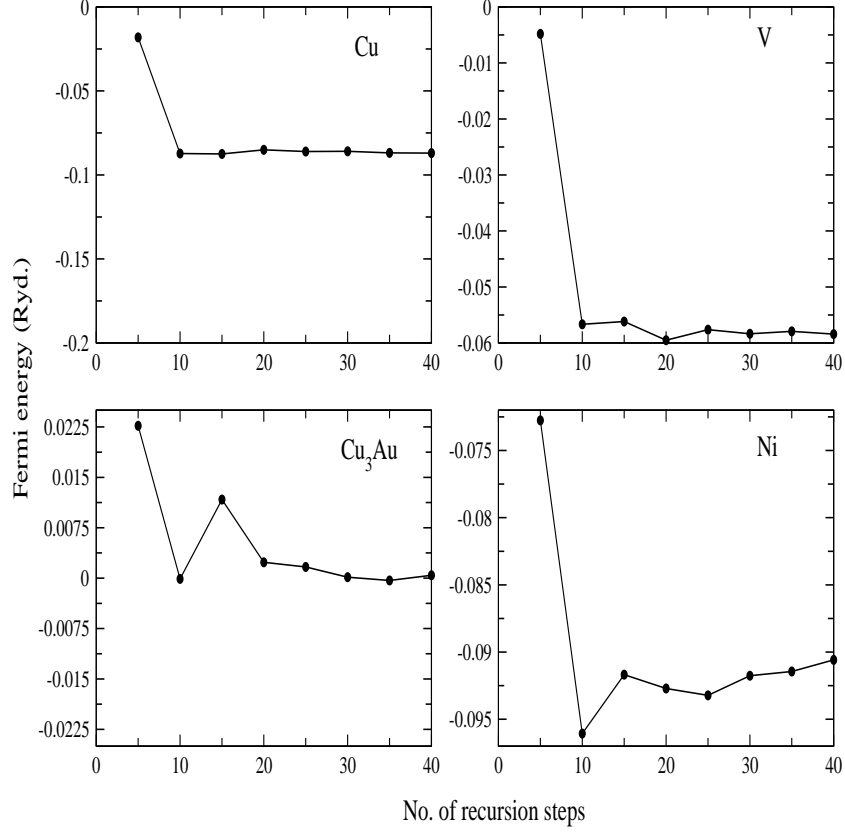


Figure 5. The convergence with recursion step of the Fermi energies of Cu, Cu–3Au, Ni and V

If the first N continued fraction coefficients are exact, that is in case we carry out our recursion on a N -shell neighbour map upto N steps and then terminate, the error in the various moment functions are :

$$\delta M_k(E) = + \sum_{n=N}^{\infty} \left\{ \delta a_n A_n^{(k)}(E) + \delta b_{n+1} B_n^{(k)}(E) \right\} \quad (7)$$

Where,

$$A_n^{(k)}(E) = \frac{2}{b_1} \int_{-\infty}^E P_{n+1}(E') \mathcal{Q}_{n+1}(E') (E')^k n(E') dE'$$

$$B_n^{(k)}(E) = \frac{4}{b_1} \int_{-\infty}^E P_{n+1}(E') \mathcal{Q}_{n+1}(E') (E')^k n(E') dE'$$

From this expression and equation(6) we can obtain an expression for the overall error

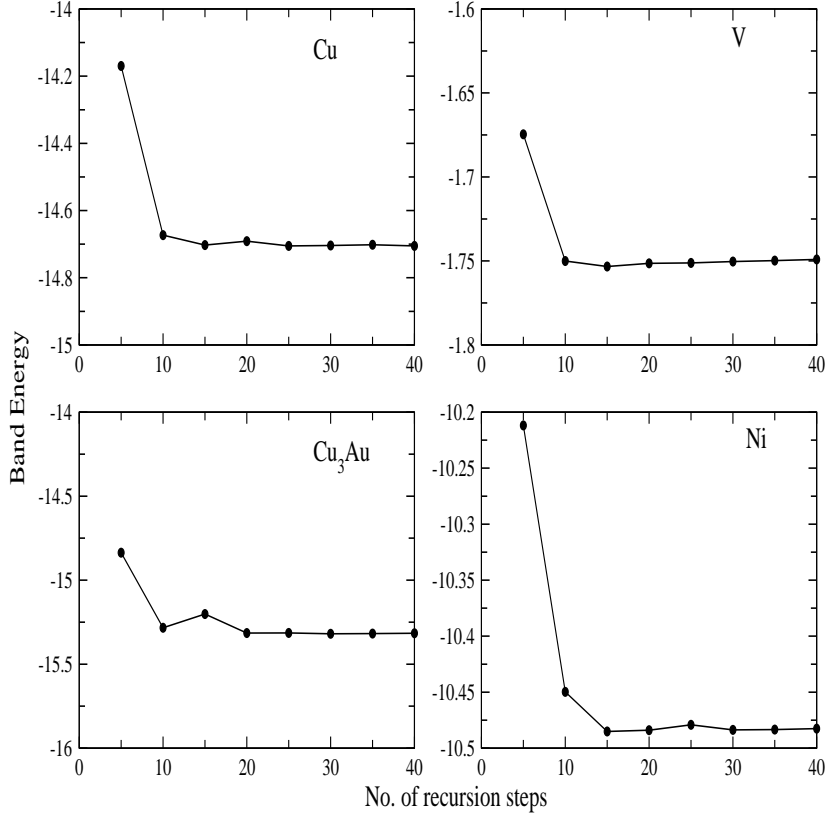


Figure 6. The convergence with recursion step of the band energies of Cu, Cu₃Au, Ni and V

in the moments. Numerical results for the errors in the moment functions are shown in figure 4. The convergence in Fermi and band energies with number of recursion steps are shown in figures 5 and 6.

These are calculated on a 20 shell neighbour map and upto 40 steps in recursion. The figures clearly illustrate the convergence of the procedure with increasing recursion steps, as surmised by Haydock. As expected the higher moments converge more rapidly. The rapid convergence of higher moments is at the basis of the reproduction of most of the density of states shape in an approximate recursion procedure. It should be noted, however, that we carry out recursion beyond 40 steps, very soon the procedure becomes unstable. This instability arises due to two sources : (i) we have carried out recursion on a 20 shell neighbour-map. As we go beyond 20 steps of recursions, finite size effects begin to show up. Numerically till 40 steps these errors are tolerable. Beyond 45 they lead to instability. We can control this by increasing the size of the neighbour-map. (ii) Numerical cumulative errors lead to the loss of orthogonality in the recursion generated

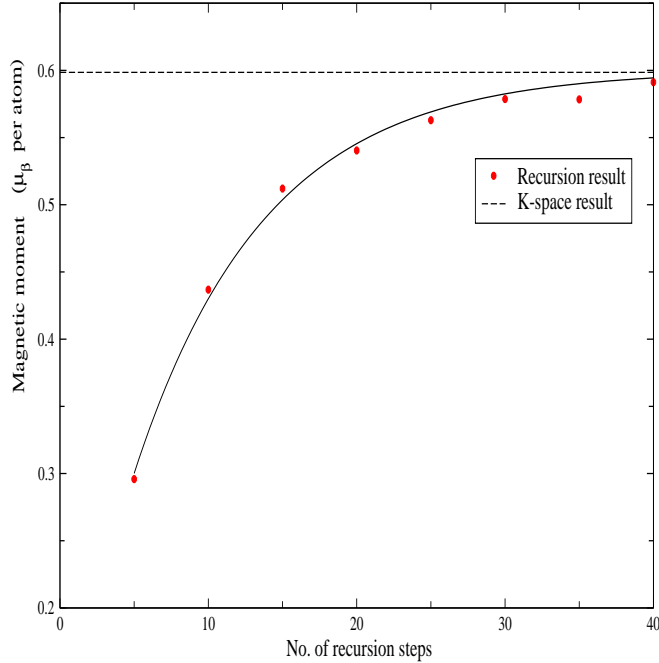


Figure 7. The convergence with recursion step of the magnetic moment of Ni

basis. This can be controlled by deliberately orthogonalizing after every 20 steps or so. In the presence of disorder, the sharp structures in the density of states are smoothed by finite life-time effects. The convergence of the higher moments is even more rapid. The above analysis in ordered systems is therefore in a *worst scenario* situation.

Figure 7 shows the convergence of the magnetic moment of Ni as a function of the number of recursion steps towards the value $0.6 \mu_B$ obtained from k -space techniques. Magnetic moment is a physical quantity which is very sensitive to the errors in numerical approximations. The figure shows that within 35-40 recursion steps on a 20 shell real-space map, the magnetic moment has converged within our error tolerance.

It is evident from the above analysis that the size of the neighbour map and the number of recursion steps required can vary from system to system. For every situation, we have to carry out this error analysis before we can rely on our numerical results with a degree of satisfaction.

3. Calculations on a model system

Before we carry out calculations on a real alloy, let us first apply our formalism to a toy model in order to understand the effects of partial disordering. We shall consider a

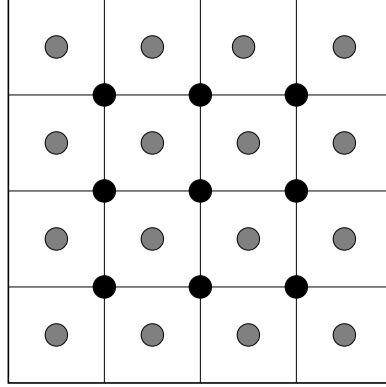


Figure 8. Ordered atomic arrangement on a square lattice for a $A_{50}B_{50}$ alloys

50-50 AB alloy ordered first on a square lattice as shown in figure 8 and only s -states on this atomic arrangement. The Hamiltonian in a tight-binding basis set is then,

$$H = \sum_i \epsilon_{i\alpha, i\alpha'} \mathcal{P}_{i\alpha, i\alpha'} + \sum_{\{ij\}} t_{i\alpha, j\alpha'} \mathcal{T}_{i\alpha, j\alpha'}$$

where $\{ij\}$ denotes that i and j are nearest neighbour cells on the lattice, α is 1 or 2 according to whether we are referring to the corner atoms or central atoms in a square unit cell (dark and light atoms in figure 8). If we consider only the nearest neighbour overlaps at a distance $a/\sqrt{2}$ where a is the square lattice constant, the diagonal and off-diagonal terms of the Hamiltonian are (referring to figure 9)

$$\begin{aligned} \epsilon_{i\alpha, j\alpha'} &= \begin{pmatrix} \epsilon & t \\ t & \epsilon \end{pmatrix} \\ t_{i\alpha, j\alpha'} &= \begin{pmatrix} 0 & 0 \\ t & 0 \end{pmatrix} && r_i - r_j \text{ are in the } (10) \text{ and } (01) \text{ directions} \\ t_{i\alpha, j\alpha'} &= \begin{pmatrix} 0 & t \\ 0 & 0 \end{pmatrix} && r_i - r_j \text{ are in the } (10) \text{ and } (01) \text{ directions} \end{aligned}$$

The ordered lattice has a density of states which has a central band gap with integrable infinite Van Hove singularities at the two internal band edges, two kink singularities within the band and the usual square-root singularities at the external band edges. As expected, the density of states is symmetric about the band centre $\bar{\epsilon} = 0.5$. This is shown in figure 10.

The density of states for the perfectly disordered lattice, where each lattice site is occupied by either A or B atom with probabilities proportional to their concentrations, is shown in the figure 11. Disorder washes away the Van Hove singularities and the central band gap is filled up. The results are identical to a disordered square lattice with lattice vectors $(a/\sqrt{2}, 0)$ and $(0, a/\sqrt{2})$.

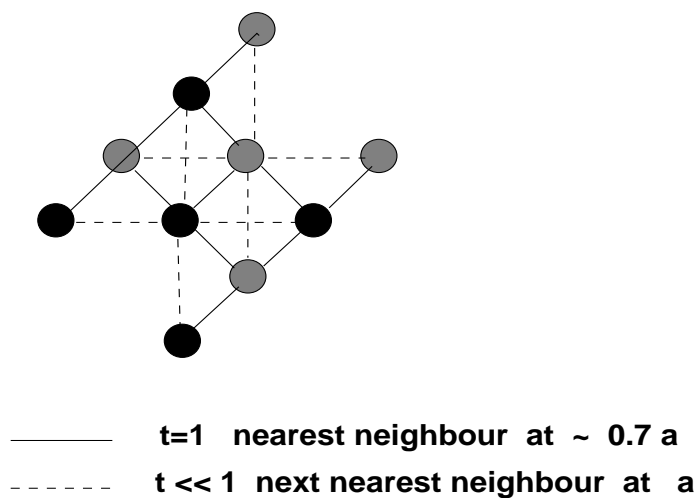


Figure 9. Nearest neighbour overlaps for a central cell in a square lattice with lattice constant a units

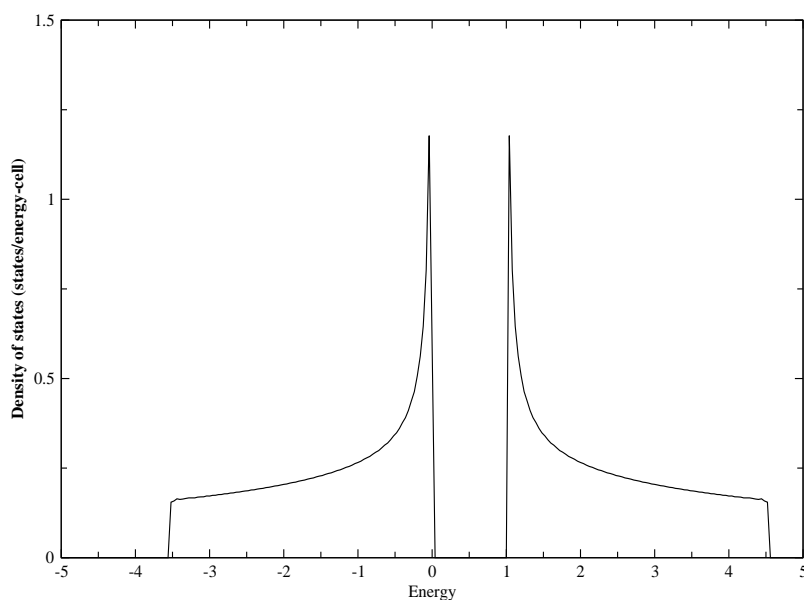


Figure 10. Density of states for the perfectly ordered lattice

The next figure 12 shows the density of states and Fermi energies for the partially disordered half-filled alloys at just off-stoichiometric compositions (49.5-50.5) and (50.5-49.5). Disorder washes out the Van Hove singularities, although vestiges of the kink singularities remain. The signature of the internal infinite singularities show up as peaks, but disorder fills up the internal band gap. The band-edge square-root singularities remain as artifacts of the termination procedure. Loss of stoichiometry weights the two ‘bands’ differently leading to a loss of symmetry about the band centre.

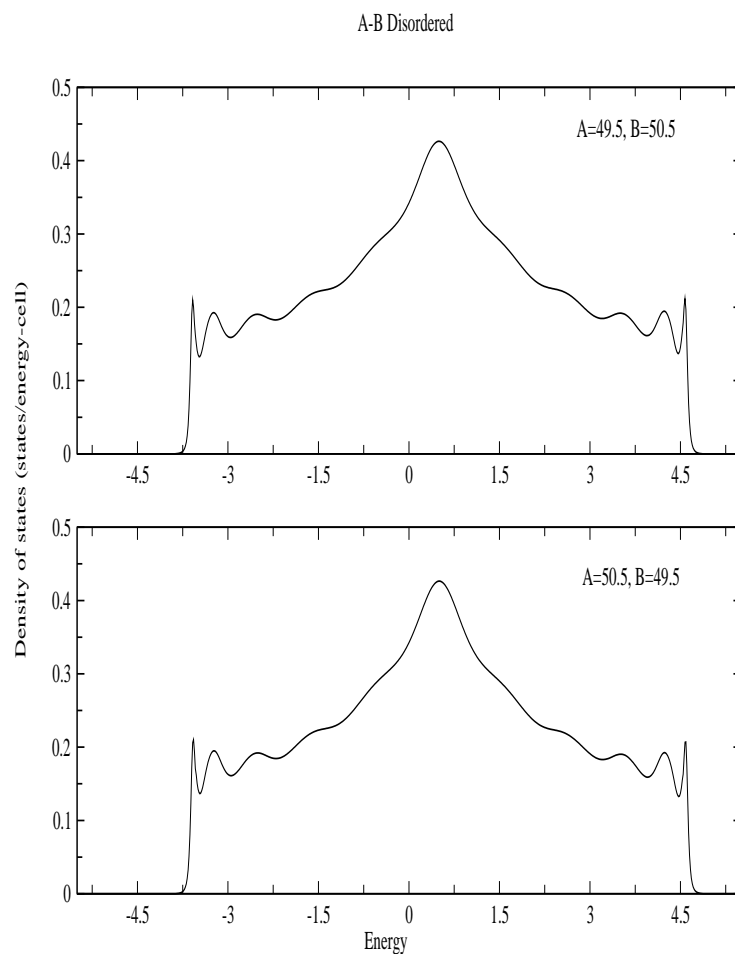


Figure 11. Partial Density of states (states/energy-cell) for the A and B atoms (top,bottom) for a completely disordered alloy at different off-stoichiometric compositions

The figure 13 shows the band energy for the partially ordered alloys. There is a jump at the stoichiometric composition with the band energy for the ordered alloy falling half way between the two branches. This jump can be understood by carefully examining the graphs on the left panels and right panels of the figure 13. The band energy represents the average energy (centre of gravity) of the portion of the graph to the left of the Fermi-energy. The density of states on the left panel have greater weight below the Fermi energy as compared to those on the right panel, ensuring the band energy to be more negative for the compositions shown on the left panels. The sudden jump is the result of the Fermi energy shifting across the pseudo band-gap as we cross the 50-50 composition and including the high peak at $E=0$, which shifts the average energy to higher values. The specific behaviour of the band energy depends sensitively on the

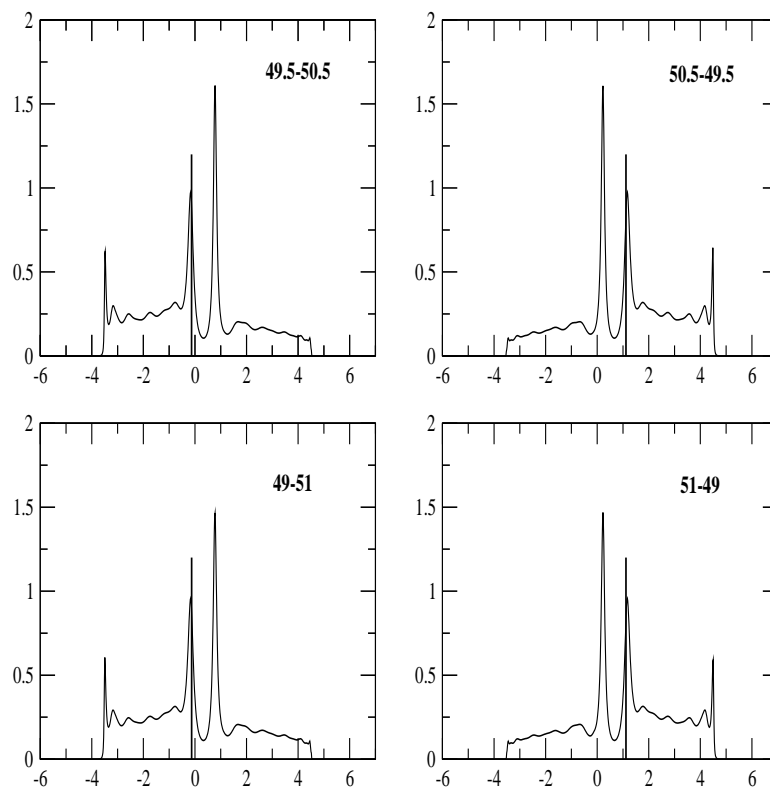


Figure 12. Density of states (states/energy-cell) for partially disordered alloy, at different off-stoichiometric compositions

features of the density of states. The specific behaviour for our toy model may not obtain for realistic alloy systems.

In contrast, the behaviour of the band energy with composition for the fully disordered alloy is smooth, reflecting the smooth behaviour of the density of states without any internal band gaps. The figure indicates that for compositions to the left of the 50-50 stoichiometric one, the alloy prefers to be partially ordered. At 50-50 the ordered alloy is stable for our toy model. While for compositions to the right of 50-50 the alloy stabilizes in the completely disordered phase.

4. Remarks and Conclusion

In this communication we have first proposed a generalization of the ASR for partially ordered binary alloy systems. Partial ordering of the type where disorder in different

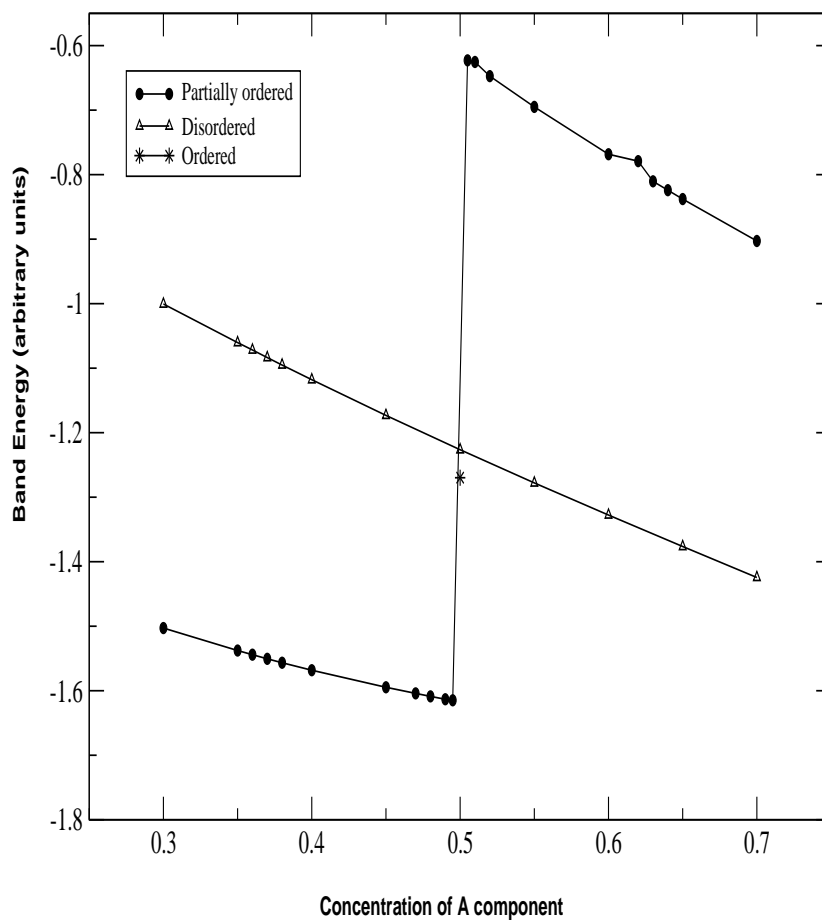


Figure 13. Band energies for the partially ordered, fully ordered and fully disordered alloys at stoichiometric (50-50) and nearby off-stoichiometric compositions

sublattices are different has been studied in particular. We have analyzed the convergence of the recursion technique in the worst scenario case of no disorder and have argued that disorder smoothens out structure in the density of states, so that for disordered alloys the convergence of the moments is even faster. Finally we have studied a model system, in order to understand the effects of partial disordering. We are now in a position to apply our formalism to realistic alloy systems. This will be the subject matter for a subsequent communication.

References

- [1] Andersen O.K. in *Computational Methods in Band Theory*, eds. P.M. Marcus, J.F. Janak and A.R. Williams (Plenum, New York, 1971), p.178.
- [2] Andersen O.K. and Jepsen O., *Phys. Rev. Lett.* **53** 2571 (1984)
- [3] Andersen O.K., Jepsen O. and Krier G. in *Lectures on Methods of Electronic Structure Calculations*, eds. V. Kumar, O.K. Andersen and A. Mookerjee (World Scientific, Singapore, 1994), p.63.
- [4] Ghosh S., Das N., Mookerjee A., *J. Phys.: Condens. Matter* **9** 10701(1997)
- [5] Haydock R. *J. Phys. A: Math. Gen.* **7** 2120 (1972)
- [6] Haydock R., Heine V. and Kelly M. J., *J. Phys. C: Solid State Phys.* **5** 2845 (1972)
- [7] Haydock R., Heine V. and Kelly M. J., *Surf. Sci.* **38** 139 (1973)
- [8] Haydock R. *Solid State Physics* (Academic Press, New York) **35** (1988)
- [9] Arnold W. T., Haydock R. (private communication) (2001)
- [10] Kudrnovský., Bose S. K., Anderson O. K., *Phys. Rev.* **B 43** 4613 (1991)
- [11] Mookerjee A., *J. Phys. C: Solid State Phys.* **6** L205 (1973)
- [12] Mookerjee A., 1973 *J. Phys. C: Solid State Phys.* **6** 1340 (1973)
- [13] Saha T. , Dasgupta I. and Mookerjee A., *J. Phys.: Condens. Matter* **6** L245 (1994)
- [14] Saha T. , Dasgupta I. and Mookerjee A. , *J. Phys.: Condens. Matter* **8** 1979 (1996)
- [15] Saha T. and Mookerjee A., *J. Phys.: Condens. Matter* **10** 2179 (1997)